

NASA-CR-203133

NTG

NA60-2825

7N-70-OR

018234

HIGH PRESSURE VAPOR TRANSPORT OF  $\text{ZnGeP}_2$ :  
I. PARAMETER EVALUATION

S. Fiechter

Hahn-Meitner-Institut  
Department of Physical Chemistry  
Glienicke Strasse 100, D-14109 Berlin

R. H. Castleberry, N. Dietz and K. J. Bachmann  
Department of Materials Science and Engineering

H. T. Banks, K. Ito, J. S. Scroggs and Hien Tran  
Department of Mathematics  
North Carolina State University, Raleigh, North Carolina

Abstract

$\text{ZnGeP}_2$  crystals and epilayers can be grown by chemical vapor transport using phosphorus or hydrogen chloride as transporting agent. The limiting factor in the transport rate is the volatility of germanium which has a seven order of magnitude smaller partial pressure than elemental zinc. Excluding oxygen using carbon films inside the growth vessels and employing a nitrogen shroud in the furnace tube also transport of  $\text{ZnGeP}_2$  will be obtained when phosphorus is used as transport agent. Optical absorption measurements above show the presence of absorption band head systems which cannot be explained by the absorption lines of  $\text{P}_2$ ,  $\text{P}_4$ ,  $\text{PO}$  or  $\text{GeO}$ . These new bands are also present in the vapor above  $\text{ZnGeP}_2$  but not above  $\text{ZnP}_2$ . The experimental findings have been simulated by thermochemical calculations taking into account estimated values for the vapor species  $\text{GeP}$ .

I. Introduction

$\text{ZnGeP}_2$  crystallizes in the chalcopyrite structure which can be inferred from the zincblende lattice by doubling the unit cell of  $\text{ZnS}$  and ordering the cation sublattice. In the tetragonal unit cell a small distortion occurs in the direction of the c-axis which substantially affects the optical properties of this compound semiconductor. The material is of interest in context of its non-linear optical properties and can be applied as optical parametric oscillator or for frequency mixing. For this reason, thick films or crystals of high transparency are in demand, which can be grown from the vapor phase.

The dissociation pressure of the ternary chalcopyrite  $\text{ZnGeP}_2$  amounts to 3.5 bars at the melting point at 1295 K [2]. In the last contribution to this conference series [1] we directed attention to the sensitive change of this equilibrium pressure with composition of the condensed phase. Therefore, close control of the partial pressures of the constituting elements and their gaseous compounds during vapor growth is necessary.

In this paper we discuss vapor phase transport experiments of  $\text{ZnGeP}_2$  in oxygen free environment using phosphorus or hydrogen chloride as transport agent. It is assumed that germanium as well as zinc could form volatile phosphorus species. To detect new phosphorus bearing gas species, optical absorption spectroscopy of the vapor phases over  $\text{ZnGeP}_2$ ,  $\text{ZnP}_2$  and  $\text{GeP}$  has been performed. The results are compared with thermochemical calculations using the free energy minimization method described by Ericson [3].

II. Transport Experiments

In order to distinguish the conditions of multiphase from those for single phase transport under exclusion of deleterious effects of residual oxygen contamination of the vapor atmosphere experiments

employing selected vapor composition have been performed using carbonized quartz tubes which were first etched in aqua regia, rinsed with distilled water, dried and finally baked under vacuum at 1223 K for 24 hours to minimize the concentration of water and OH-groups in the walls of the tubes. Prior to sealing under vacuum with a quartz plug the ampoules were filled with about 1 g pre-synthesized  $\text{ZnGeP}_2$ . To fix the phosphorus vapor pressure appropriate amounts of  $\text{Zn}_3\text{P}_2$  and P were added. The ampoules had a diameter of 10 mm and a length of 150 mm. A temperature differences of  $\Delta T = 1308\text{-}1243$  K was applied for 168 hours using a resistance heated furnace. After cooling, the ampoules were opened under  $\text{N}_2$  atmosphere and the products characterized by x-ray diffractometry, scanning electron microscopy (SEM) and energy dispersive x-ray analysis (EDX). Typical results are given in table I.

Table I Results of transport experiments using P and HCl as transporting agents.

No.	Ingots	Ampoule	Transported Phases
III/2	$\text{ZnGeP}_2$ (1.1631 g) $\text{Zn}_3\text{P}_2$ (3.8 mg) P (47.1 mg)	heated, carbonized HCl added (35 kPa)	<u><math>\text{ZnGeP}_2</math></u> , $\text{ZnP}_2$ (5%) $\text{Zn}_3\text{P}_2$ (5%) GeP or Ge (1%) transport rate $\sim 3$ mg/hr
III/3	$\text{ZnGeP}_2$ (1.12338 g) $\text{Zn}_3\text{P}_2$ (2.9 mg) P (50 mg)	heated, carbonized HCl added (35 kPa)	<u><math>\text{ZnGeP}_2</math></u> , $\text{ZnP}_2$ (2%) $\text{Zn}_3\text{P}_2$ : (5%) GeP or Ge (2%) transport rate $\sim 3$ mg/hr
III/4	$\text{ZnGeP}_2$ (0.935 g) $\text{Zn}_3\text{P}_2$ (2.3 mg) P (47.3 mg)	heated, no graphite layer	<u><math>\text{ZnP}_2</math></u> , <u><math>\text{ZnGeP}_2</math></u> <u><math>\text{Zn}_3\text{P}_2</math>: Ge</u> (GeP or Ge) transport rate $\sim 2$ mg/hr
III/5	$\text{ZnGeP}_2$ (1.054 g) $\text{Zn}_3\text{P}_2$ (2.6 mg) P (49.6 mg)	heated, carbonized double wall	<u><math>\text{ZnP}_2</math></u> , <u><math>\text{ZnGeP}_2</math></u> <u><math>\text{Zn}_3\text{P}_2</math>: Ge</u> (GeP or Ge) transport rate $\sim 2$ mg/hr

In all experiments transport of  $\text{ZnGeP}_2$  was observed. The main transported phases in experiments without HCl were  $\text{ZnP}_2$ ,  $\text{Zn}_3\text{P}_2$  and  $\text{ZnGeP}_2$ . The presence of Ge or GeP can be inferred from the XRD patterns (see fig. 1.a). Heating of the tube under vacuum and/or the presence of a carbon film inside the ampoule wall diminishes the oxygen content so that no  $\text{Ge}_x\text{O}_x$  species can be formed. Nevertheless, the transport of  $\text{ZnGeP}_2$  without halogen proceeds at a high rate. This points to the fact that other volatile Ge species have to be present in the vapor phase. The specific stoichiometry of the  $\text{Ge}_x\text{P}_y$  species that are responsible for the observed transport in the experiments III/4 and III/5 is not known at this time.

The x-ray diffractograms of the transported material, shown in figs. 1.a and 1.b, can be indexed as  $\text{ZnGeP}_2$  (JCPDS 33-1471),  $\text{ZnP}_2$  (JCPDS 23-748),  $\text{Zn}_3\text{P}_2$  (JCPDS 22-1021), Ge (4-545) and GeP (21-348).

SEM images of a polished sample of experiment III/5 reveal that at least three phases are present (see figure 2). A dark phase ( $\text{ZnP}_2$ ), a dark grey phase ( $\text{ZnGeP}_2$ ) and a light grey phase ( $\text{Zn}_3\text{P}_2$ ) containing 2 mole% Ge. The element concentrations were measured by microprobe analysis (EDX). To separately study the chemical transport behavior of GeP 10<sup>-2</sup> mole Ge and P were placed in a BN-boat sitting in an evacuated and sealed quartz ampoule ( $l = 250$  mm,  $\phi = 20$  mm) and treated in a temperature

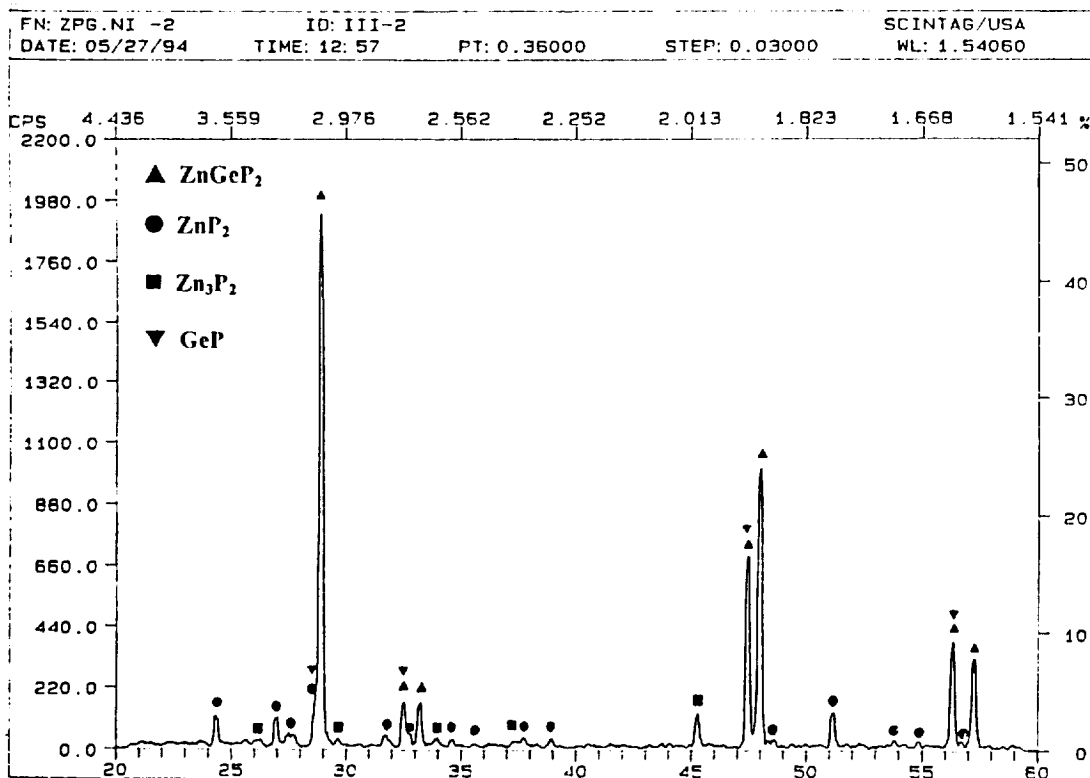


Figure 1.a: x-ray diffractogram of transported material from experiment III/2. Besides  $\text{ZnGeP}_2$  small amounts of the phases  $\text{ZnP}_2$ ,  $\text{Zn}_3\text{P}_2$ , Ge or  $\text{GeP}$  are present. ( $\text{CuK}\alpha$  radiation,  $\lambda = 1.5406 \text{ \AA}$ ).

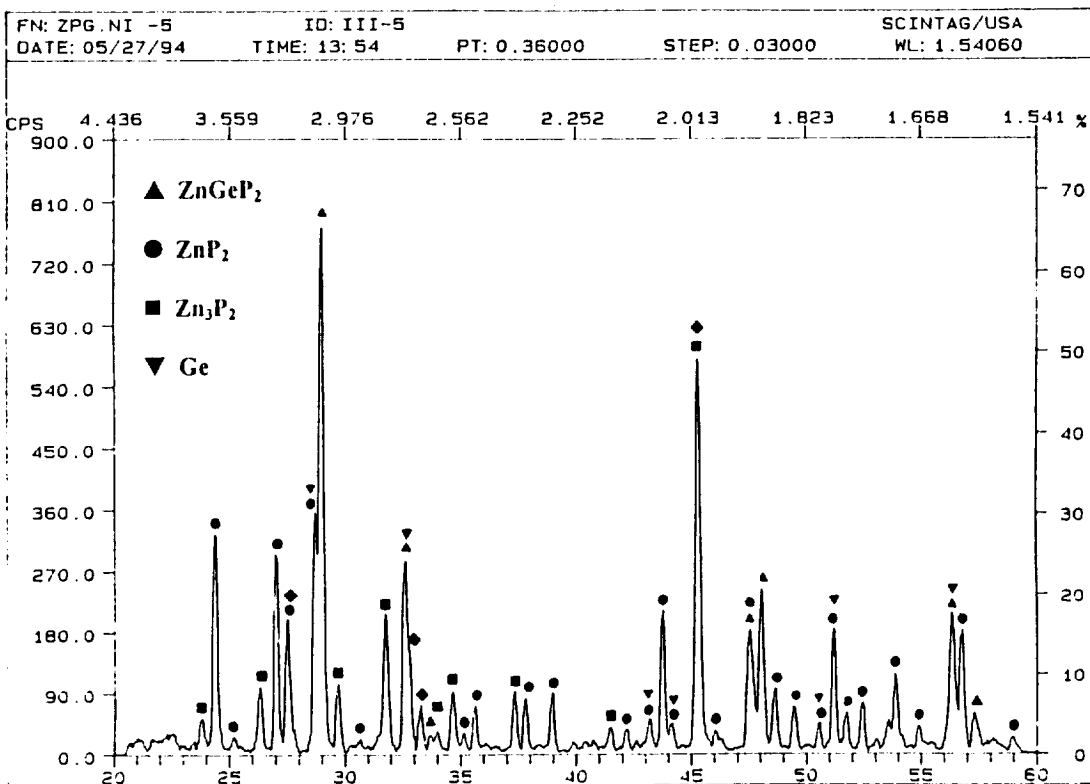


Figure 1.b.: X-ray diffractogram of transported material from experiment III/5. Main phases:  $\text{Zn}_3\text{P}_2$ ,  $\text{ZnP}_2$ ,  $\text{ZnGeP}_2$  and Ge and  $\text{GeP}$  possible. ( $\text{CuK}\alpha$  radiation,  $\lambda = 1.5406 \text{ \AA}$ ).

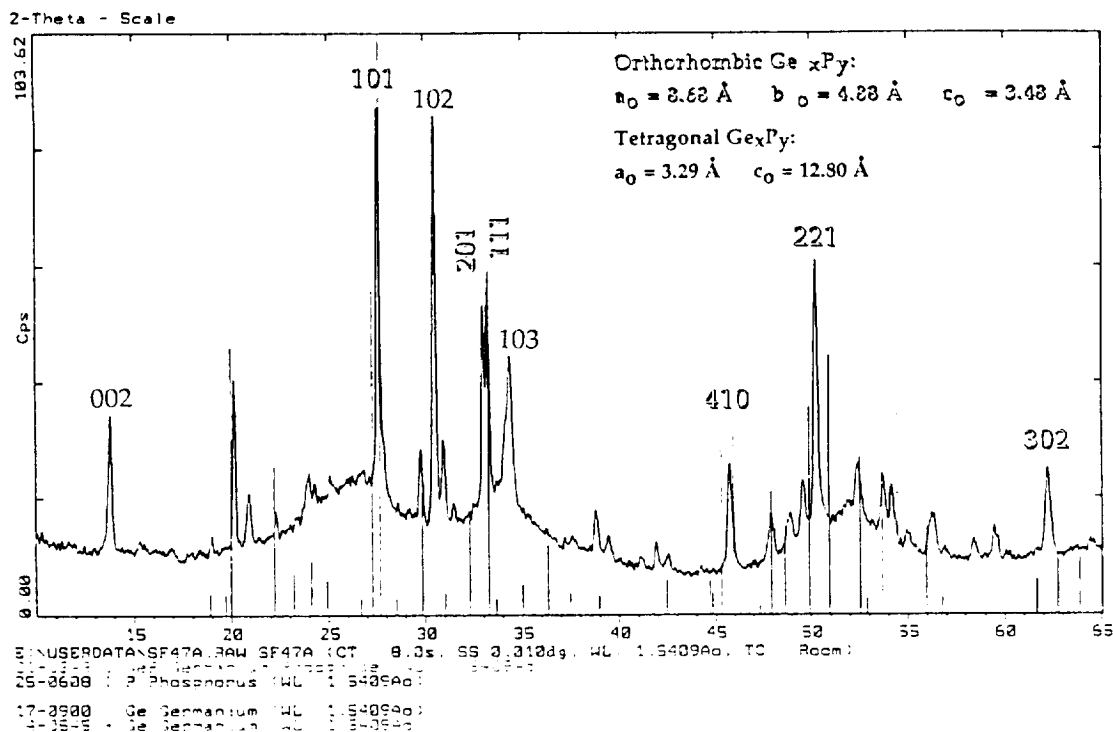


Figure 1.c: X-ray diffractogram of transported material from a chemical vapor transport experiment with GeP using phosphorus as transporting agent. Present phases: GeP, Ge and unknown other germanium phosphides of orthorhombic and tetragonal symmetry. ( $\text{CuK}\alpha$  radiation,  $\lambda = 1.5409 \text{ \AA}$ ).

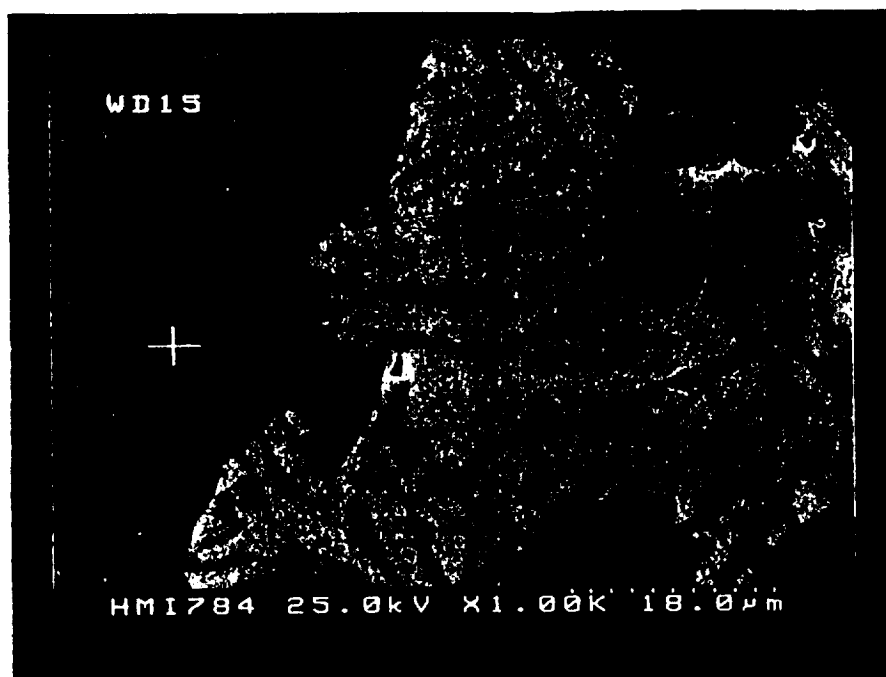


Figure 2: Scanning electron micrograph of a polished sample from transported material in experiment III/4. Black phase:  $\text{ZnP}_2$ , dark grey phase:  $\text{ZnGeP}_2$ , light grey phase:  $\text{Zn}_{2.8}\text{Ge}_{0.2}\text{P}_2$ .

difference from  $\Delta T = 1173 - 673$  K. Within two days a black layer has been formed consisting of orthorhombic and tetragonal germanium phosphides (fig. 1.c).

Composition and structural analysis of the vapor species in the system Zn-Ge-P can be analysed by optical measurements in the vapor phase. In the following chapter we present results from optical absorption measurement.

### III. Optical absorption spectroscopy

Optical emission and absorption spectroscopy is a method to study molecular structures of gas species and to obtain their thermochemical data. It can also be used to quantitatively measure element concentrations in the vapor phase. (e.g. by Atomic Absorption Spectrometry AAS). Although it is difficult to identify new gas species from such spectra the absorption or emission lines can be utilized to distinguish different gas species in the vapor phase. In our experiments the pressures in the analyzed gas volumes range from mbar up to several bars. We compare the absorption spectra of the elements with the absorption behaviour over the condensed binary and ternary compounds. In the wavelength range from 180 to 1000 nm vibronic spectra have been described, in which transitions occur from rotational/vibrational states of one electronic state to rotational/vibrational states of another electronic state [4].

The setup to measure the absorption bands in the vapor phases over  $\text{ZnGeP}_2$ ,  $\text{ZnP}_2$  and GeP is illustrated in figure 3. The equipment consists of a two zone furnace with integrated isothermal furnace liners (Dynatherm) to guarantee a uniform temperature profile for the quartz glass cuvettes of 50, 100 mm length and 10 mm diameter. The temperature was controlled by PID temperature controllers (Eurotherm 808), the temperature was monitored by two NiCr/Ni thermocouples. The cuvettes were mounted on top of a V-shaped rim which was mounted at the ends on holders fixed on a vibrational isolated table. To change the cuvettes the furnace was mounted on a slide which enabled a reproducible positioning of the cuvettes in every run. As light source a xenon lamp (ORIEL 7340, Xe 6253, 150 W) was employed. To guide the light through the heated quartz glass cuvettes (Hellma Inc.) and to focus the transmitted light onto the entrance slit of a monochromator (ISA HR 320) a system of quartz lenses (UV grade) was used. The light intensity was detected at the exit slit of the monochromator by a photomultiplier tube (Hamamatsu 522; operation voltage  $U = 1200$  V using an Ortec HV supply) and amplified with a pre-amplifier (Keithley 602). To improve the signal to noise ratio the light was chopped with 334 Hz (Chopper: Stanford Research SR 540) and phase sensitively amplified by a lock-in amplifier (EG&G 5206). To overcome the so-called schlieren effect, which also contributes the noise level of the measurement by air turbulences in the heated furnace core, the cuvettes to be measured were placed between two empty quartz glass cuvettes. To investigate the absorption behavior, about 50 mg of red phosphorus,  $\text{ZnGeP}_2$ ,  $\text{ZnP}_2$  and GeP, respectively, were filled into the evacuated and sealed cuvettes. The results are shown in the figures 4.a to c. Figure 4.a shows a compilation of the transmission curves over  $\text{ZnGeP}_2$  at 807 K, GeP at 881 K and  $\text{ZnP}_2$  at 773 K. The different temperatures of the cuvettes take into account the temperature dependence of the vapor pressures and were chosen to yield comparable absorption intensities.

The absorption curves of  $\text{ZnGeP}_2$ , GeP and  $\text{ZnP}_2$  show a common minimum at about 245 nm and a transmission maximum in the wavelength range from 240 to 200 nm. At higher wavelengths a continuous increase of transmission is typical for all spectra. This general curve shape can be explained by the transmissivity of the quartz glass used (lenses and cuvettes) and the higher light intensity of the Xe-lamp at higher wavelengths. As reference the transmission curve of a 10 mm thick specimen of GE type 124 fused quartz is shown in figure 4.b. Additional minima in the curves are typical features of the vapor species over the related compounds. Due to the moderate resolution of the used monochromator (0.05 nm) compared to vacuum spectrographs with an resolution of 0.001 nm only band heads could be detected.

a)  $\text{ZnP}_2$ : two spectra have been measured at 773 and 723 K (figure 4.c). The transmission curve exhibits two strong absorption maxima at 290 and 296.7 nm and shows high absorption at wavelengths smaller than 260 nm for the 773 K spectrum, which are not explained by absorption bands of gaseous Zn or  $\text{Zn}_2$

[5, 6]. Since homogeneous evaporation of  $\text{ZnP}_2$  has been described in the literature [7] volatile zinc phosphides exists in the vapor phase. However, the pronounced absorption maxima observed over  $\text{ZnP}_2$  are not present in the vapor phase over  $\text{ZnGeP}_2$  (not shown in figure 4.a and 4.f). This means that within the detection limit of our experiments no zinc phosphide species are present in the equilibrium above the chalcopyrite.

b) GeP: Comparing the number of absorption maxima of P, GeP and  $\text{ZnGeP}_2$  in the wavelength range from 190 to 250 nm (figs. 4.d, 4.e and 4.f) GeP exhibits the most complex spectrum. The analysis of the line positions shows that this spectrum consists of absorption lines of  $\text{P}_2$  [5, 8, 9] and at least of one additional vapor species (see Table II), whose line positions relate to the most prominent absorption maxima in the range from 180 to 245 nm.

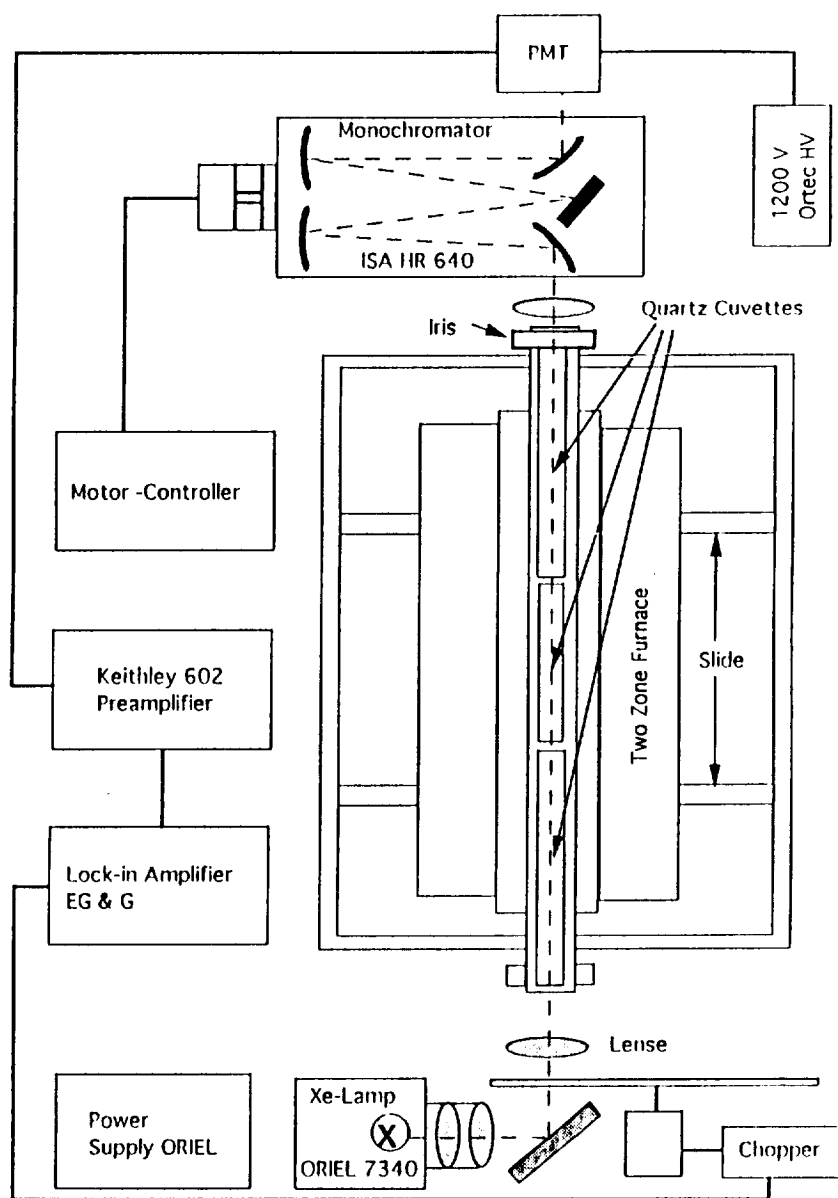


Figure 3: The experimental set-up to measure transmission curves of the equilibrium vapor over  $\text{ZnGeP}_2$ ,  $\text{ZnP}_2$ , GeP and P (red).

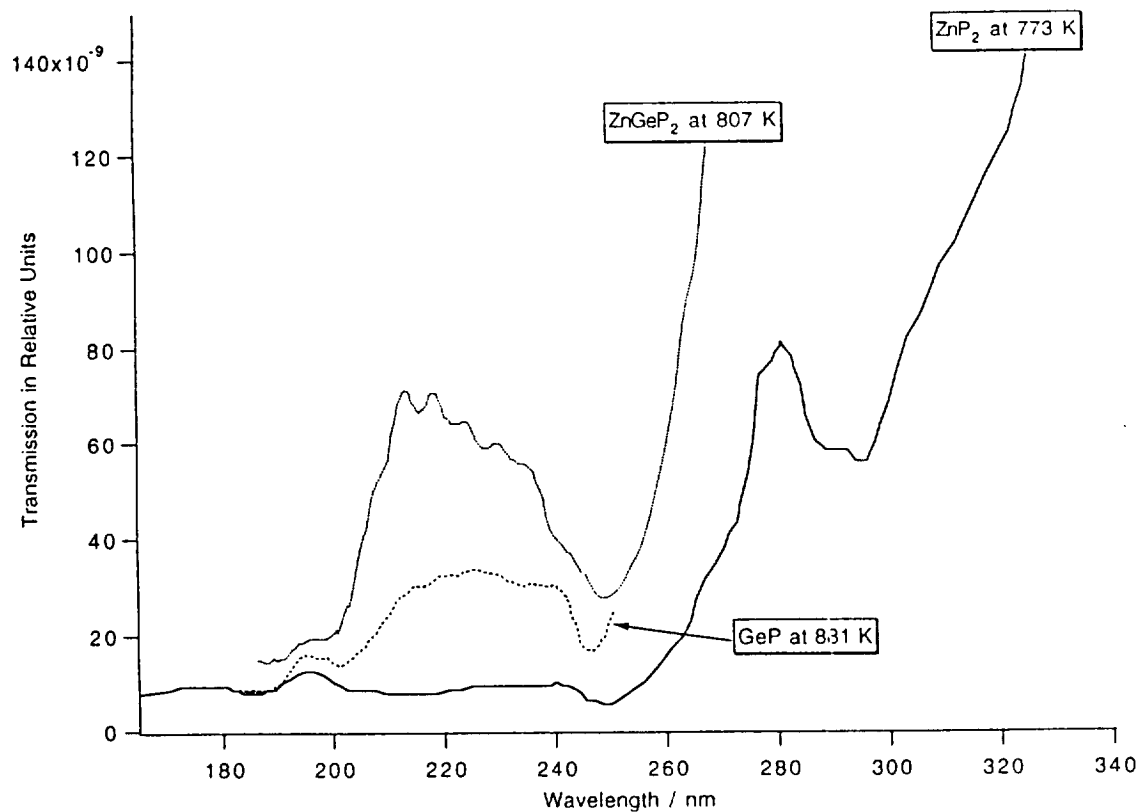


Figure 4.a: Transmission curves of the equilibrium vapor phases over ZnGeP<sub>2</sub>, ZnP<sub>2</sub>, GeP and P (red).

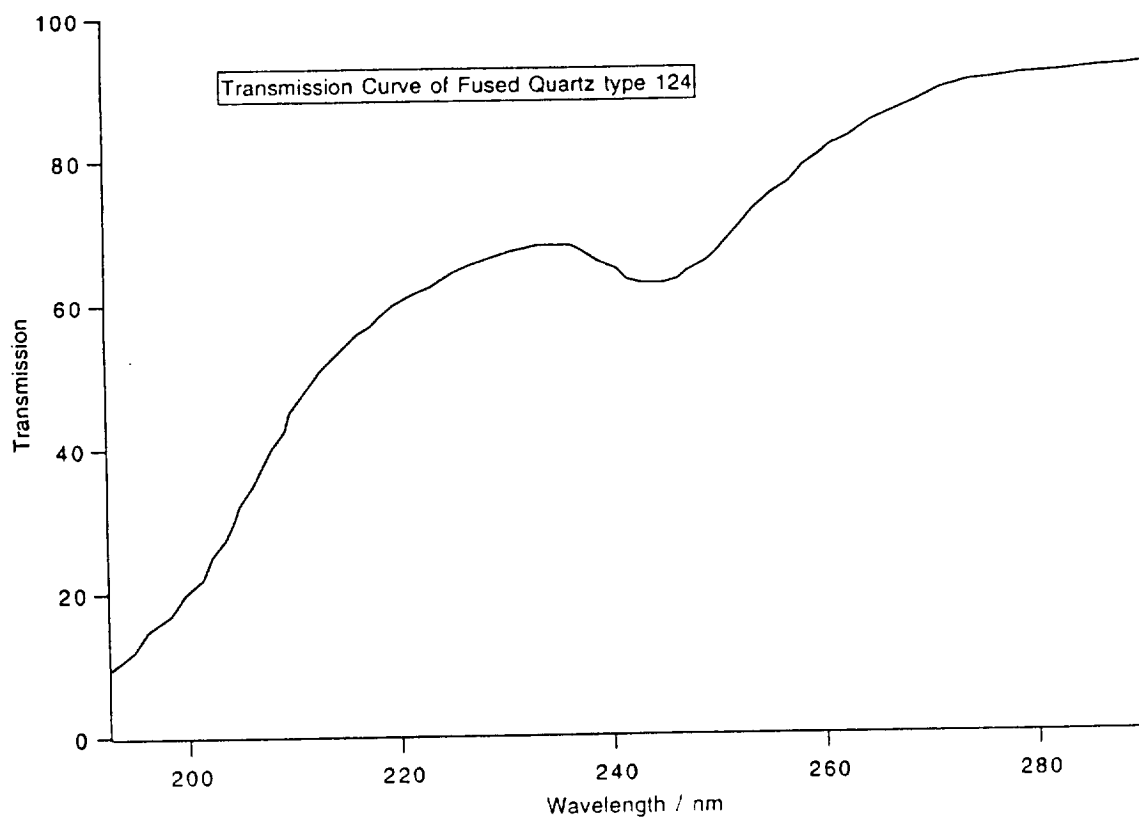


Figure 4.b: Transmission curve of a 10 mm thick fused quartz plate (GE Quartz, type 124)

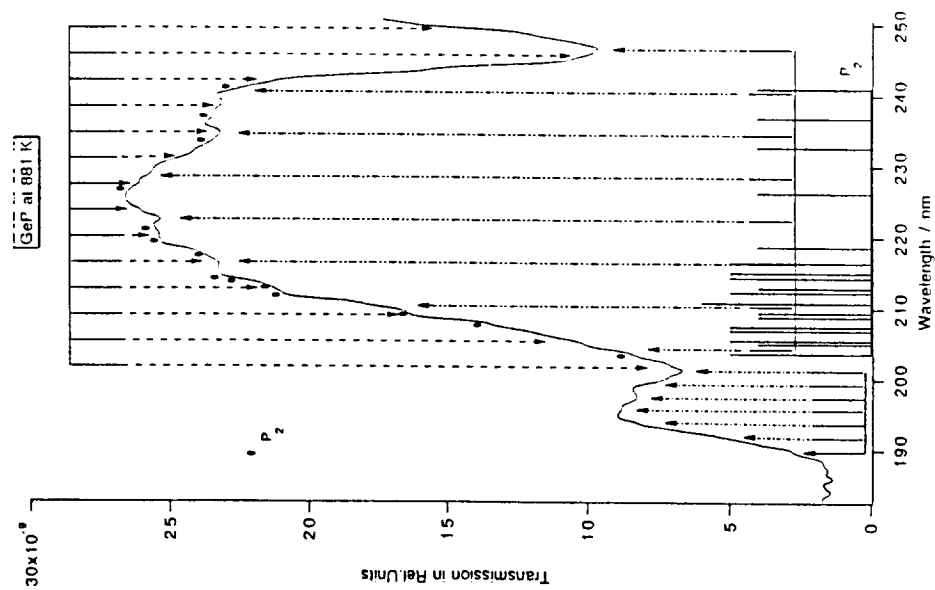


Figure 4.c: Transmission curve of the equilibrium vapor phase over ZnP<sub>2</sub>.

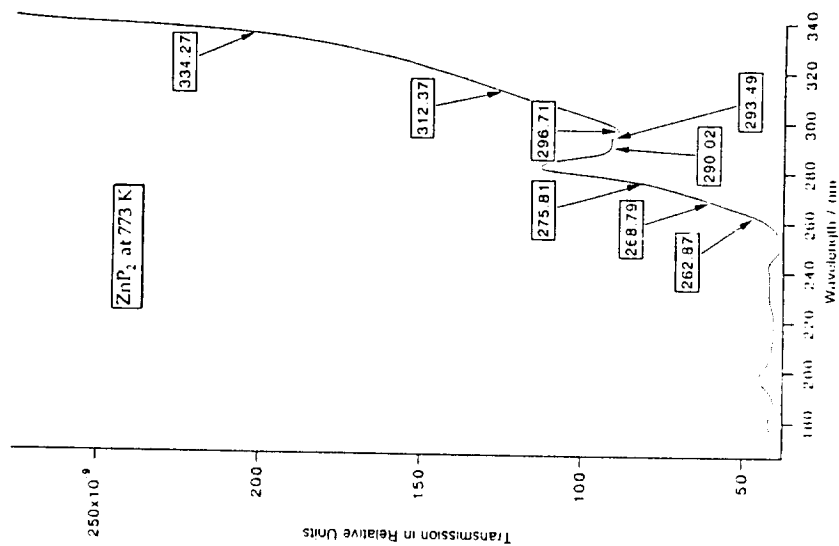


Figure 4.d: Transmission curves of the equilibrium vapor phase over GeP.



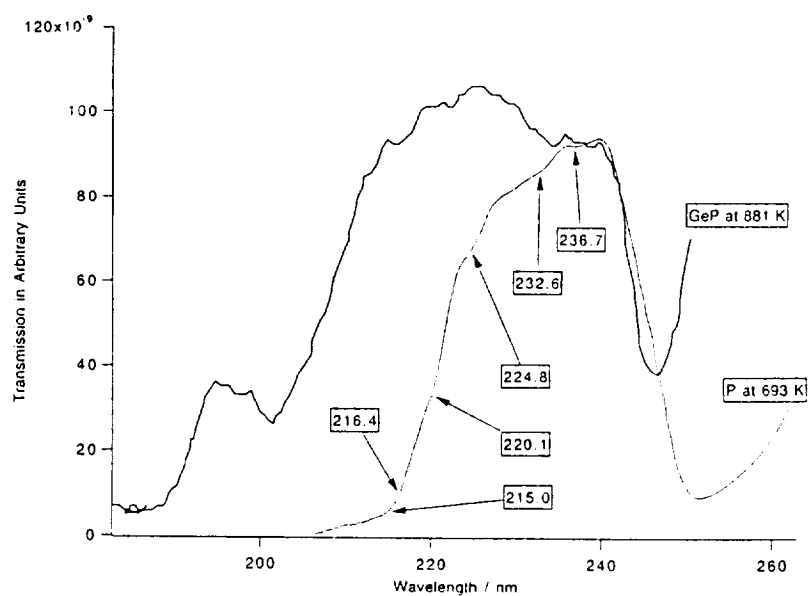


Figure 4.e: Transmission curves of the equilibrium vapor phase over GeP and P (red).

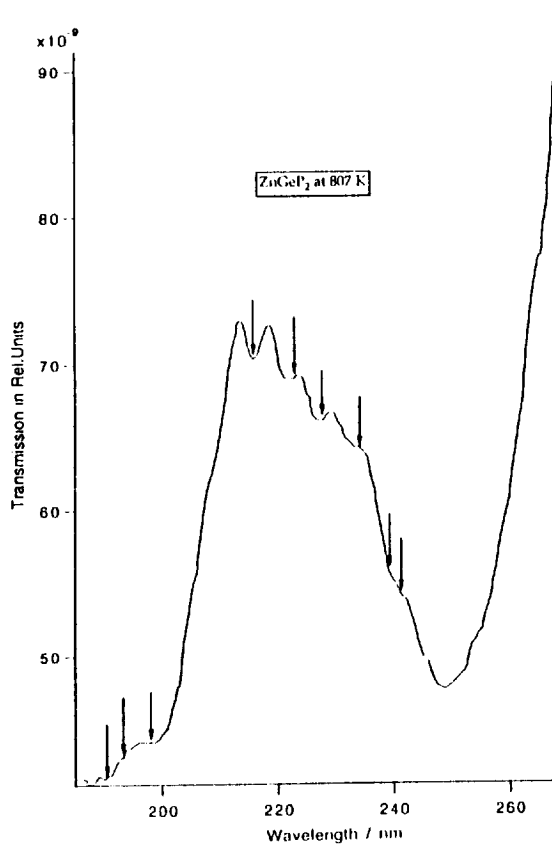


Figure 4.f: Transmission curves of the equilibrium vapor phase above ZnGeP<sub>2</sub>. The positions of the arrows mark the position of Ge<sub>x</sub>P<sub>y</sub> band heads.

In order to check the vibrational analysis of a band system the attempt has been made to set out the wave numbers of the absorption maxima in a Deslandres table [4]. Three progressions have been found which are depicted as line grids in figure 4.d together with the line positions of  $P_2$ . The analysis is correct if the wave numbers of corresponding bands in different  $v'$  (excited states) and  $v''$  (ground states) progressions, respectively, are constant. Tentatively the grid with narrow distances could be assigned as a  $v'$  progression for  $v'' = 0$  while the other two grids belong to higher  $v'$  and  $v''$  progressions. For thermochemical calculations the existence of the gaseous species GeP has been assumed.

Table II Positions of the absorption heads in figure 4.d with possible progressions I, I and III (P:  $P_2$  lines).

Absorption lines of $P_2$ in nm	Absorption lines of Ge $P_x$ in nm
	III: 190.3, 194.1, 195.4, 197.0, 198.0, 200.0. 201.5 I
203.6	
205	
205.5	205.35 I
206.9	
207.49	207.58 P
208.83	
209.43	209.8 I, P
210.81	211.07 P 212.02 I
212.26	
212.86	212.98 P 213.62
214.3	214.26 P
215.0	
	215.94 II
216.4	216.8 P 217.78 I, II
218.64	218.74 P
220.14	220.34 I, P 222.59 II 223.55 I
226.16 I	226.11 I 227.08 I 228.37 II 231.59 I
	232.55
232.65	234.16 I, II
	236.73 P
236.76	238.98 I
	240.91 P, II
240.99	241.56 243.2 244.51 I 246.77 II

#### IV. Heat of formation of $\text{ZnGeP}_2$

In the last contribution to preceding conference [1] we inferred the heats of formation of  $\text{ZnP}_2$ ,  $\text{Zn}_3\text{P}_2$  and  $\text{ZnGeP}_2$  from equilibrium vapor pressure measurements (Table III). The values for  $\text{ZnP}_2$  and  $\text{ZnGeP}_2$  differ by  $\sim 2$  kcal/mole. This result is in agreement with Differential Thermal Analysis DTA measurements that we employed to study the reaction of  $\text{ZnP}_2$  with Ge to form  $\text{ZnGeP}_2$ . Figure 5 shows a typical result. Mainly endothermic contributions to the reaction heat occur which are about 2 kcal/mole smaller than the heat of fusion of  $\text{ZnGeP}_2$  ( $\Delta H^m = 8.8$  kcal/mole).

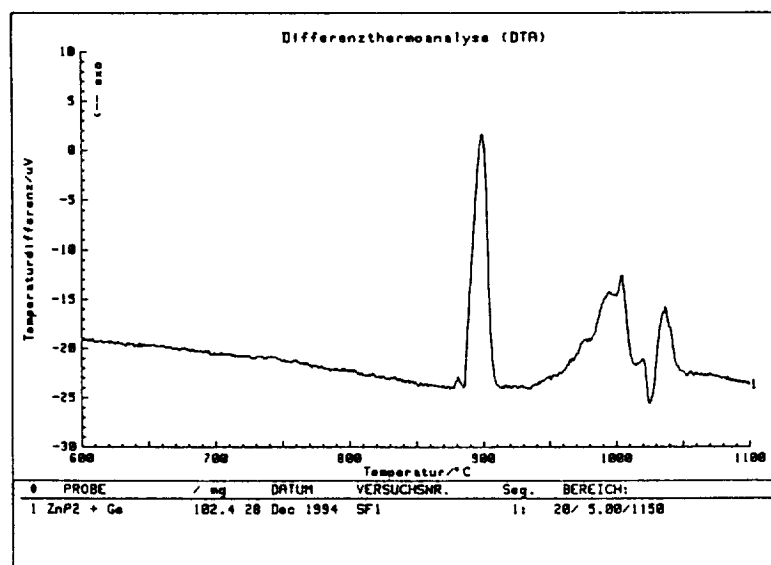


Figure 5. Differential Thermal Analysis DTA curve of reaction  $\text{ZnP}_2 + \text{Ge} = \text{ZnGeP}_2$

#### V. Phase relations, predominance area diagram and vapor phase composition

Figure 6 depicts the Gibbs phase triangle for the system Zn-Ge-P. The GeP binary shows five condensed phases but only GeP and presumably  $\text{GeP}_2$  are stable under normal pressure conditions (65 kbar) [10]. IV-V compounds of composition  $\text{AB}_2$  ( $A = \text{Si, Ge}$ ;  $B = \text{P, As}$ ) crystallize in two modifications: in a high pressure modification of pyrite structure [10] and an low pressure orthorhombic structure [11]. In the x-T diagram of Ge-P the existence of  $\text{GeP}_2$  is not mentioned [10, 11]. In accord with the Gibbs phase rule, triangular subfields are defined in the Zn-Ge-P composition field. The solid phases coexisting in equilibrium for any composition in these subfields are given by the corner compounds and elements.

With the thermochemical data, summarized in Table III, thermochemical calculations using the free energy minimization technique were carried out. One result is the predominance area diagram depicted in figure 7, showing the stability field for  $\text{ZnGeP}_2$  as a function of the partial pressures  $P_{\text{P}}$  and  $P_{\text{Zn}}$ . The number of phases found in the XRD pattern from experiment III/3 (figure 1.a), especially the presence of Ge and/or GeP, shows that the system was not in equilibrium. This may be due to the fact that the heats of formation of  $\text{ZnGeP}_2$  and  $\text{ZnP}_2$  do not differ significantly so that Ge and  $\text{ZnP}_2$  can occur as metastable

Table III Thermochemical data used for free energy minimization calculations. The dimensions of the standard heat of formation  $\Delta H_f^\circ$ , heat of fusion  $\Delta H_{fu}$  or heat of evaporation  $\Delta H_e$  are kcal/mole, for the standard entropies  $S_f$  and molar heats  $c_p$  cal/mole deg.

Element/ Compound	$\Delta H_f^\circ$	$S_f^\circ$	$c_p = A + B \cdot 10^{-3} \cdot T + C \cdot 10^5 \cdot T^{-2}$		
	$\Delta H_{fu}$ $\Delta H_e$		A	B	C
P (red)	0.00	5.45	4.051	3.559	-
P <sub>4</sub> (white)	16.68	39.28	18.28	15.12	-
P (l)	17.31	-	25.168	-	T>317 K
<b>P<sub>4</sub> (g)</b>	<b>30.77</b>	<b>66.89</b>	<b>19.562</b>	<b>0.162</b>	<b>-3.213</b>
<b>P<sub>2</sub> (g)</b>	<b>40.68</b>	<b>52.11</b>	<b>8.675</b>	<b>0.191</b>	<b>-0.994</b>
Zn (s)	0.00	9.943	5.096	2.782	0.13
Zn (l)	1.75	-	7.495	-	-
<b>Zn (g)</b>	<b>31.15</b>	<b>38.451</b>	<b>4.965</b>	-	-
ZnCl <sub>2</sub> (s)	-99.13	26.62	14.290	8.994	-
ZnCl <sub>2</sub> (l)	2.474	-	2.588	-	-
<b>ZnCl<sub>2</sub> (g)</b>	<b>-63.839</b>	<b>66.185</b>	<b>14.74</b>	<b>-1.03</b>	-
Ge (s)	0.00	7.425	5.577	0.931	-0.25
Ge (l)	8.82	-	6.596	-	T>1210 K
<b>Ge (g)</b>	<b>89.34</b>	<b>40.1</b>	<b>7.038</b>	<b>-0.873</b>	<b>0.76</b>
GeH <sub>4</sub> (g)	21.68	51.89	14.939	5.276	-5.166
<b>GeP (s)</b>	<b>-0.13</b>	<b>14.6</b>	<b>10.84</b>	<b>2.7</b>	<b>-1.25</b>
<b>GeP (g)</b>	<b>28.4</b>	<b>44.43</b>	<b>12.34</b>	-	-
GeO (s)	-50.3	11.9	9.543	3.497	-
GeO (g)	-10.99	53.49	8.92	0.0239	-1.3685
Ge <sub>2</sub> O <sub>3</sub> (g)	-112.	75.1	20.	-	-
<b>Ge<sub>3</sub>O<sub>3</sub> (g)</b>	<b>-212.</b>	<b>99.3</b>	<b>32.</b>	-	-
GeCl (g)	174.36	58.72	10.314	-0.532	-1.18
<b>GeCl<sub>2</sub> (g)</b>	<b>-40.84</b>	<b>70.63</b>	<b>13.818</b>	<b>0.052</b>	<b>-0.88</b>
<b>ZnP<sub>2</sub></b>	<b>-24.15</b>	<b>14.4</b>	<b>17.01</b>	<b>3.997</b>	<b>0.65</b>
<b>Zn<sub>3</sub>P<sub>2</sub></b>	<b>-38.65</b>	<b>36.2</b>	<b>30.15</b>	<b>6.225</b>	<b>-0.36</b>
<b>ZnGeP<sub>2</sub></b>	<b>-26.3</b>	<b>28.22</b>	<b>24.65</b>	<b>3.5</b>	<b>-4.0</b>

phases. The predominance area diagram allows the equilibrium between  $\text{ZnGeP}_2$ ,  $\text{ZnP}_2$  and  $\text{Zn}_3\text{P}_2$  as found in experiment III/5 (fig. 1.b). Calculating the phase equilibria under experimental conditions (Table I) the triple point was found 20 K below the experimental value of 1243 K. Above this temperature  $\text{ZnGeP}_2$  and  $\text{ZnP}_2$  were stable, the equilibrium pressure at 1240 K amounted to 3.4 bar. In the presence of HCl higher pressures have to be expected. They ranged from 6.8 to 5.8 bar. It was found that mainly  $\text{ZnGeP}_2$  is stable in presence of a small amount of Ge which is in agreement with the experimental findings.

The calculations employing estimated thermochemical data for gaseous species  $\text{GeP}$  (Table III) show a dominance in the formation of  $\text{ZnGeP}_2$ , and a small amount of  $\text{ZnP}_2$ . However, the experiment showed the transport of  $\text{ZnGeP}_2$ ,  $\text{Zn}_3\text{P}_2$  and  $\text{ZnP}_2$  in comparable amounts. This points to the fact that the stability of the assumed vapor species  $\text{GeP}$  was over estimated. Further measurements such as mass spectroscopic analysis are in progress to yield more insight in the vapor phase composition above  $\text{GeP}$ .

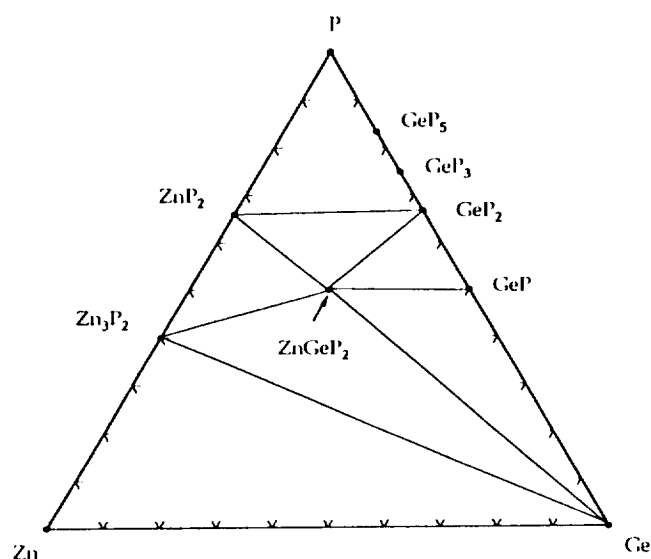


Figure 6. Gibbs phase triangle of the system  $\text{ZnGeP}_2$ .

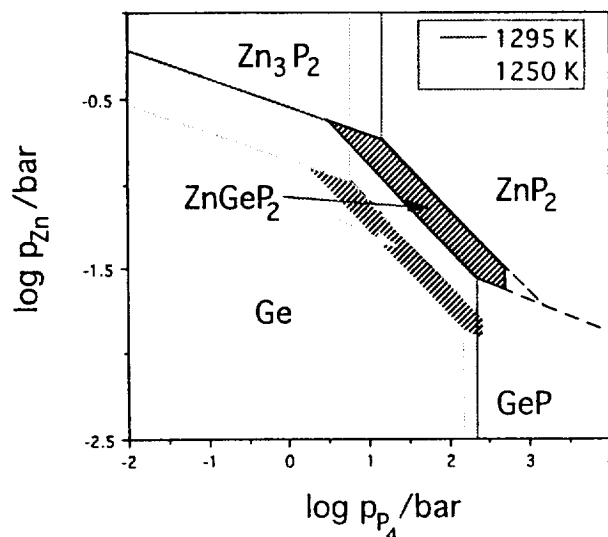


Figure 7. Predominance area diagram for the system Zn-Ge-P

#### VI. Conditions of single phase $\text{ZnGeP}_2$ transport

he vapor composition and transport rate described in table I that lead to multiphase transport, we have performed experiments under slightly changed conditions resulting in single phase  $\text{ZnGeP}_2$  transport. This requires working with smaller temperature gradients, typically  $< 4 \text{ K/cm}$  ( $\Delta T = 1300\text{-}1290 \text{ K}$ ) and short transport distances. A typical vapor composition for single phase transport is:  
 $[\text{Zn}] = 6.27 \times 10^{-7} \text{ mol/cm}^3$ ,  $[\text{P}] = (3.254 \times 10^{-5} \text{ mol/cm}^3)$  and  $[\text{HCl}] = (1.3 \times 10^{-5} \text{ mol/cm}^3)$

#### VII. Concludig remarks

$\text{ZnGeP}_2$  can be grown by chemical vapor transport using phosphorus as transporting agent. The presence of volatile  $\text{Ge}_x\text{P}_y$  species can be concluded from careful analysis of the absorption spectra measured in the vapor phases above  $\text{ZnGeP}_2$  and  $\text{GeP}$  in the wavelength range from 190 to 260 nm. Due to the small

difference in the heats of formation between  $\text{ZnGeP}_2$  and  $\text{ZnP}_2$  a close space vapor transport geometry is recommended to grow crystals or layers of  $\text{ZnGeP}_2$ .

### Acknowledgement

The authors (S. F. and H. C.) would like to thank Mr. J. Pirollo (NCSU) for quartz glass blowing, Dr. J. Lilie (HMI) for his technical assistance evaluating the absorption spectra, Mrs. I. Simonson (NCSU) and Mr. K. Diesner (HMI) for doing XRD measurements. This work was supported in part by the National Aeronautics and Space Administration Grant NAWG-2865 and the National Science Foundation DMR-9202210.

### References

1. S. Fiechter, R. H. Castleberry, G. Wood, K. J. Bachmann, H. T. Tran, K. Ito and J. S. Scroogs, "High pressure vapor transport of binary and ternary compound semiconductors," Proceedings of the 6. International Symposium on Experimental Methods for Microgravity Materials Science, R. Schiffmann (ed.), (TMS, Warrendale PA, 1994) 93-100.
2. A. S. Borshchevskii, and T. M. Shantsovoi, "Pressure and Composition of the Vapor above Semicoinductive  $\text{ZnGeP}_2$ ," Inorg Chem., 11 (1975), 1853-1855.
3. G. Ericson, and K. Hack "ChemSage - A Computer Program for the Calculation of Complex Chemical Equilibria," Metallurgical Transactions B, 21B (1990), 1013-1023.
4. G. Herzberg, The Spectra and Structures of Simple Free Radicals (Dover Publications, New York, 1971).
5. R. W. B. Pearse, and A. G. Gaydon, The Identification of Molecular Spectra (John Wiley & Sons, New York, 1963).
6. R. C. Weast, and M. J. Astle, CRC Handbook of Chemistry and Physics (CRC Press, Boca Raton, Florida, 1981), Line Spectra of the Elements, E-205 to E-334.
7. V. B. Lazarev, V. J. Shevchenko, S. F. Marenkin, and G. Magomedgadghiev, "The Growth of Large Tetragonal  $\text{CdP}_2$  and  $\text{ZnP}_2$  Crystals," J. Crystal Growth, 38 (1977), 275-276.
8. A. Jakowlewa, "Fluoreszenz and Absorption des Phosphordampfes," Z. P., 69 (1931), 548-564.
9. G. Herzberg, L. Herzberg, and G. Milne, "On the Spectrum of the  $\text{P}_2$  Molecule," Canad. J. Res., A18 (1940) 139-143.
11. P. C. Donohue, and H. S. Young, "Synthesis, Structure and Superconductivity of New High Pressure Phases in the System Ge-P and Ge-As," J. Solid State Chem., 1 (1970) 143-149.
12. T. Wadsten, "The Crystal Structures of  $\text{SiP}_2$ ,  $\text{SiAs}_2$  and  $\text{GeP}$ ," Acta Chem. Scand., 21 (1967) 593-594.
13. T. B. Massalski, Binary Alloy Phase Diagrams (American Society for Metals, Metals Park, Ohio, 1990) Vol. 2, p. 1978-1979.